

## Properties of bulk $\delta$ -TiN<sub>1-x</sub> prepared by nitrogen diffusion into titanium metal

Walter Lengauer

*Institute for Chemical Technology of Inorganic Materials, Technical University of Vienna, Getreidemarkt 9, A-1060 Vienna (Austria)*

(Received February 13, 1992)

### Abstract

Compact titanium nitride ( $\delta$ -TiN<sub>1-x</sub>) within the compositional range TiN<sub>0.53</sub>-TiN<sub>1.00</sub> was prepared by a diffusion process and several of its properties were investigated as a function of composition. The microstructures showed an equiaxial polygonal grain boundary arrangement with some individual pores in the centre, particularly for the substoichiometric samples, probably as a result of the diffusion process. The samples exhibited good homogeneity. The microhardnesses  $HV_{0.1}$  (at 0.98 N) and  $HV_{0.3}$  (at 2.94 N) both show maxima for TiN<sub>0.67</sub> of 24.4 and 23.8 GPa respectively, whereas TiN<sub>1.00</sub> has values of 17.2 and 17.0 GPa respectively. The crack formation resistance measured by the Palmqvist method is of the order of  $45 \text{ kJ m}^{-2}$  and was found to be independent of the nitrogen content. The nitrogen sublattice occupancy was determined by density measurements. Within the accuracy of the results the titanium sublattice is fully occupied throughout the homogeneity range of TiN<sub>1-x</sub> whereas the nitrogen sublattice is occupied according to the stoichiometry TiN<sub>1-x</sub>. The electrical conductivity at room temperature increases with increasing nitrogen content from  $0.48 \times 10^4 \Omega^{-1} \text{ cm}^{-1}$  for TiN<sub>0.53</sub> to  $3.74 \times 10^4 \Omega^{-1} \text{ cm}^{-1}$  for TiN<sub>1.00</sub>. The rate of oxidation increases with increasing nitrogen content at both 800 and 1000 °C for samples of composition TiN<sub>>0.67</sub>. Samples of composition TiN<sub><0.67</sub> showed nitride phase transformation and a more peculiar oxidation behaviour. The colour of  $\delta$ -TiN<sub>1-x</sub> changes from metallic grey for TiN<sub>0.53</sub> to golden yellow for TiN<sub>1.00</sub>, with the first perceptible brownish yellow tinge at TiN<sub>0.77</sub>.

### 1. Introduction

Among the transition metal nitrides the f.c.c. phase TiN<sub>1-x</sub> has become the most interesting for use in "high tech" applications such as cermets, electronic and optical devices and protective coatings [1].

According to the phase diagram of the Ti-N system, which is shown in Fig. 1 as constructed from the compilation of Wriedt and Murray [2] supplemented by results from recent diffusion couple investigations [3], the homogeneity region of the f.c.c. phase  $\delta$ -TiN<sub>1-x</sub> can extend, depending on the temperature, from less than 33 to 50 at.% N. Recently, Ohtani and Hillert [4] developed a thermochemical model of the Ti-N system, including the calculation of the melting behaviour of  $\delta$ -TiN<sub>1-x</sub>.

Within the homogeneity region of  $\delta$ -TiN<sub>1-x</sub>, which can be further extended by sputter techniques [5] beyond the boundaries set by the equilibrium phase

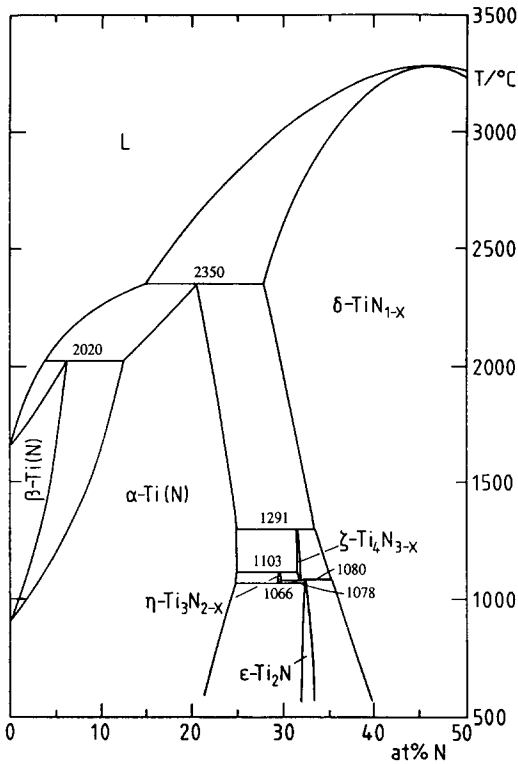


Fig. 1. Phase diagram of the Ti-N system. The literature compilation of Wriedt and Murray [2] was modified by including recent results based on diffusion couple investigations [3].

diagram, the properties of  $\delta$ -TiN<sub>1-x</sub> can vary substantially. Previous determinations of the properties of titanium nitride were usually confined to stoichiometric samples. However, in view of the technical importance of this material, its more crucial mechanical, physical and chemical properties at substoichiometric compositions are also of interest.

In several past studies dealing with the measurement of properties *vs.* composition, sintered compacts were prepared from TiN-Ti powder mixtures (see refs. 6 and 7 and references cited therein), most probably because it is the easiest technique for preparing substoichiometric titanium nitrides. This procedure may, however, result in a substantial oxygen contamination of up to several weight per cent of oxygen [6] and usually does not yield dense samples. Porosity, though, should be ruled out if basic properties of the material are to be measured without any influence from the preparative history and state.

Only in a very few studies were compact TiN<sub>1-x</sub> samples throughout the homogeneity region prepared and some of their properties investigated. With substantial apparatusive efforts Christensen and Fregerslev [8] obtained large crystals of TiN<sub>1-x</sub> by zone annealing titanium or TiN rods in an N<sub>2</sub> atmosphere. The samples were subjected to density and magnetic measure-

ments. Density measurements did not reveal any deviation from a complete occupancy of titanium in the unit cell. A similar preparation method was applied by Wolf [9], who found the same results with respect to occupancies and additionally performed several physical investigations such as superconductivity and ultrasonic measurements. However, as these authors [8, 9] stated, the zone-annealing technique does not produce perfectly homogeneous sample materials and inhomogeneities of several atomic per cent of nitrogen must be taken into account. Hence physical measurements do not necessarily yield exact physical data for property *vs.* composition relationships.

In order to investigate the more important properties of  $\delta$ -TiN<sub>1-x</sub> within the homogeneity region, the present study was performed using samples prepared by diffusion of nitrogen into titanium metal. This investigation is related to the work reported on VN [10] and NbN [11].

## 2. Experimental details

### 2.1. Sample preparation

Since TiN<sub>1-x</sub> (like all group IVb nitrides) has an extremely low nitrogen equilibrium pressure (*e.g.*  $10^{-5}$  Pa at 2000 K for TiN<sub>0.87</sub> [12]), which is one reason for its applicability as a refractory compound, it is not possible to adjust the N<sub>2</sub> equilibrium pressure in annealing experiments for the preparation of substoichiometric samples unless very high temperatures are applied. Such temperatures cause problems with contact materials. Therefore a two-step annealing process was applied. In the first step a titanium sheet (greater than 99.7 wt.% Ti, less than 0.1 wt.% O) of size  $12 \times 12 \times 1$  mm<sup>3</sup> was reacted with high purity nitrogen (zirconium foil gettered) at 1500 °C and at a pressure of about 2 bar in an autoclave with a contained gas volume. Depending on the desired composition, the reaction was stopped before complete nitridation was achieved and the nitrogen pick-up was estimated by weighing the sample. For samples near the stoichiometric composition a temperature of 1700 °C had to be applied since the nitrogen diffusivity turned out to be very low for nitrogen-rich compositions.

After this procedure the samples were introduced into a molybdenum sample holder where only one edge of each sample was in contact with the molybdenum. The samples of substoichiometric composition were heated in a purified argon atmosphere for up to 3 weeks. The temperature of this treatment had to be chosen carefully since substoichiometric TiN<sub>1-x</sub> reacts with molybdenum at high temperatures [13]. For samples at the nitrogen-poor end of the TiN<sub>1-x</sub> homogeneity region only 1350 °C could be applied, which required 3 weeks of annealing time for homogenization. The restriction in temperature is partly compensated by the higher diffusivity of nitrogen in substoichiometric TiN<sub>1-x</sub> as compared to near-stoichiometric TiN<sub>1-x</sub>.

### 2.2. X-ray diffraction and chemical analysis

After the usual phase analysis by X-ray diffraction the lattice parameter of the powdered sample material was determined using nickel-filtered Cu K $\alpha$

radiation. The four highest diffraction lines were chosen. External standardization with silicon powder was applied. Excellent  $\alpha_1$ - $\alpha_2$  line splitting indicated a good homogeneity of the samples.

Chemical nitrogen analysis of the samples was performed by means of automatic Dumas-GC analysis [14] using a Carlo ERBA CHN 1108 elemental analyser. A 1–2 mg sample of powdered material was introduced in a tin capsule and reacted with injected oxygen. Usually five parallel determinations were performed, which yielded an accuracy of better than  $\pm 1$  at.% N.

### 2.3. Metallography, hardness and Palmqvist measurements

The samples were embedded in cold-setting resin, ground and diamond polished. Finally a short polishing step using aqueous silica suspension was applied.

Vickers microhardness measurements were made with a Reichert microhardness tester using a load of 0.98 N (0.1 kp) and a Leitz microhardness tester using loads of 0.98 and 2.94 N (0.1 and 0.3 kp). The values were calibrated against a hardened steel standard for which the microhardness was known at three different loads.

Measurements of the crack lengths for obtaining crack formation resistance data by the Palmqvist method [15, 16] were performed on photographs of microhardness indentations created by the Leitz microhardness tester.

### 2.4. Density measurements

The densities of the compact nitride samples were measured by the Archimedes method. For this purpose the samples were suspended in  $\text{CHBr}_3$  for which the temperature *vs.* density function had been previously recorded. The usual precautions were made to keep the measurement error as low as possible. The steel wire used as a sample holder was introduced into the liquid to such an extent that the force measured as fictitious weight gain originating from adhesive surface tension was exactly compensated by its buoyancy. With this technique and the use of relatively large sample plates the error in the density measurements was less than 0.2%, which was checked by measuring a titanium plate (calculated 4.505, measured 4.488 g cm<sup>-3</sup>).

### 2.5. Electrical conductivity

The electrical conductivities were measured at room temperature by means of two different methods. The first is based on the measurement of inductive resistivity and was performed using a Sigmatest T apparatus from the Institute Dr. Foerster/Reutlingen, Germany. Diamond-ground sample plates were measured and the data calibrated against standard steel plates. The absolute error in electrical conductivity obtained from these measurements was estimated to be less than 3%.

Secondly, four-contact measurements were performed on prismatic samples that had been diamond cut from the plates. For this purpose four gold pins were positioned on the samples. Currents of 0.1–10 mA were passed through the samples via the outer two gold pins and the voltage drop was

measured from the two centred gold pins of fixed distance (2.705 mm). The apparatus was calibrated against NBS steel standards.

### 2.6. Oxidation experiments

In order to evaluate the oxidation behaviour, compact and diamond-ground sample plates were put in a platinum boat and heated in air at 800 and 1000 °C respectively. All samples were heated simultaneously to the given temperature. The oxidation experiments were interrupted from time to time for measurement of the weight gain. Details of the data treatment are given below.

## 3. Results and discussion

### 3.1. Microstructure

The diffusional treatment process produced samples with a slightly higher nitrogen content at the edges than at the centre of the sample. Therefore 1 mm strips were cut off the edges. Microprobe analysis of nitrogen [17] on a cross-section of the samples yielded a compositional homogeneity of better than  $\pm 2$  at.% N.

Figure 2 shows the microstructure of  $\delta$ -TiN<sub>0.53</sub>, which is the most nitrogen-deficient sample. In general a grain boundary parallel to the faces of the plate and passing through the entire sample could be observed in the centre. Only at high nitrogen contents could a few grains be observed which interrupted this grain boundary. The structure of the samples is created by symmetric diffusion whereby the  $\delta$ -TiN<sub>1-x</sub> grains obviously grow from both sides into the sample until they meet each other in the symmetry plane. The argon-annealing process does not change this structure.

It can be seen from Fig. 2 that pores occur in this symmetry plane. They were more frequent the lower the nitrogen content and scarcely visible in the sample with the highest nitrogen content. From investigations in which

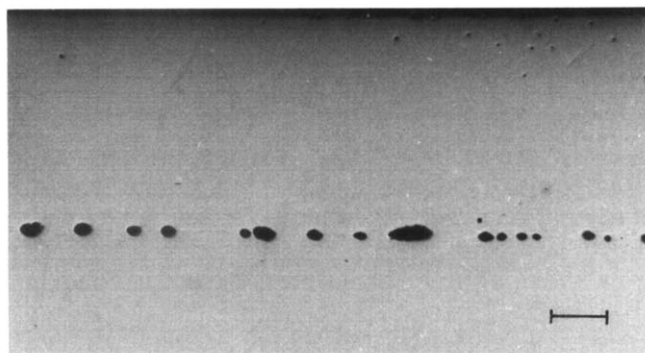


Fig. 2. Microstructure of  $\delta$ -TiN<sub>0.53</sub>, where the most frequent occurrence of pores could be observed. In the centre of the sample a large grain boundary could be seen, indicating the symmetry plane of the diffusion process. The bar represents 100  $\mu$ m.

the nitridation process was interrupted at a stage where most of the sample contained transformed  $\beta$ -Ti(N) and  $\alpha$ -Ti(N), it is known that a great number of pores first occur near the surface and in the outer  $\alpha$ -Ti(N) region [18]. When these results are compared with the microstructure in Fig. 2, the impression is obtained that these pores move with the proceeding nitridation and are finally located at the centre of the sample. The estimated porosity was much less than 1% in the case of the lowest nitrogen content, with a decrease upon reaching a single-phase sample. In stoichiometric  $\delta$ -TiN<sub>1-x</sub> the low amount of porosity can be explained by the successive filling of pores due to the material flow arising from molar volume expansion [18] and temperature induced material flow.

### 3.2. Colour, microhardness and Palmqvist values

The colour of  $\delta$ -TiN<sub>1-x</sub> changes considerably within the homogeneity region. At the nitrogen-poor end the samples showed a metallic lustre and with increasing nitrogen content they became increasingly coloured—first very slightly brownish yellow at around TiN<sub>0.77</sub>, already slightly yellow at TiN<sub>0.83</sub> and finally golden yellow at TiN<sub>0.96</sub> and TiN<sub>1.00</sub>.

The microhardness measurements are shown in Fig. 3. It can be seen that the data obtained by different microhardness testers agree well. In all three series the maximum hardness was observed in a sample of composition TiN<sub>0.67</sub>. At higher nitrogen contents the hardness decreases substantially with increasing nitrogen content. From these results it can be seen that stoichiometric TiN, which is commonly used in technical applications, is obviously not the hardest Ti–N compound available.

Unfortunately, in the literature data on the microhardness of TiN (*e.g.* refs. 19 and 20) the composition has not always been specified carefully. Most of these authors give a value of about 20 GPa. If this value is attributed to a stoichiometric composition, which is most probably the case, then it is considerably higher than observed in the present study. The difference is probably due to different grain sizes of the samples. It was shown [21] for TiC and WC that the hardness increases substantially with decreasing grain size, which can be attributed to the Hall–Petch effect. The samples of the present study had large crystallites and thus the hardness data showed no yield stress influence.

Andrievski and Spivak [22] reported on two more detailed microhardness studies which were performed on samples in the composition interval TiN<sub>0.55</sub>–TiN<sub>0.96</sub>. All cited data sets reflected generally the same behaviour—a decreasing microhardness with increasing nitrogen concentration. These data were obtained from samples which consisted of sintered powder compacts and contained up to 0.15 wt.% O.

As in TiN, a similar situation of decreasing hardness with increasing nitrogen content was observed for  $\delta$ -VN<sub>1-x</sub> [10],  $\delta$ -NbN<sub>1-x</sub> [11, 23] and  $\delta$ -TaN<sub>1-x</sub> [23], where, however, the hardness maxima are located at the nitrogen-poor boundary.

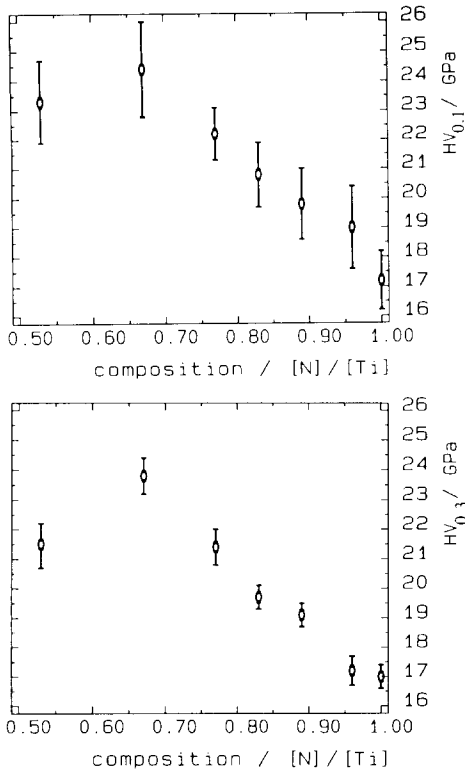


Fig. 3. Microhardness values of  $\text{TiN}_{1-x}$ : top, at a load of 0.1 kp (0.98 N) obtained with a Reichert tester (nearly identical values were obtained with a Leitz tester); bottom, at a load of 0.3 kp (2.94 N) obtained with a Leitz tester. A maximum in the  $\delta\text{-TiN}_{1-x}$  microhardness is observed at a large nitrogen deficiency at both loads.

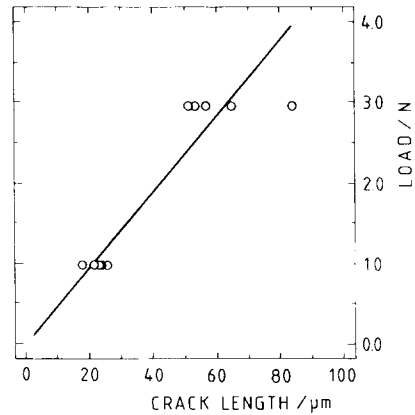


Fig. 4. Length of cracks created by Vickers indentations at loads of 0.98 and 2.94 N. The slope corresponds to a crack resistance of  $45 \text{ kJ m}^{-2}$ .

In Fig. 4 a summary of the crack length created by microhardness indentations *vs.* load is given. All investigated samples behaved similarly and no significant interdependence of crack length and composition could be detected within the homogeneity region of  $\text{TiN}_{1-x}$ . The slope of the straight line in Fig. 4 gives the crack resistance of the material, which is  $4.5 \times 10^{-2} \text{ N } \mu\text{m}^{-1}$ . In other words, the energy required for crack formation in  $\delta\text{-TiN}_{1-x}$  is, independently of composition,  $45 \text{ kJ m}^{-2}$  in the sense of a Palmqvist analysis.

### 3.3. Densities and lattice occupancies

Table 1 lists the measured densities of the investigated titanium nitrides. For the calculation of sublattice occupancies the formula

$$n_i = a^3 \rho N_A \frac{1}{M_i} m_i \quad (1)$$

TABLE 1  
Properties of the compounds investigated<sup>a</sup>

Composition [Ni]/[Ti]	Lattice parameter <i>a</i> (nm)	Microhardness		Density (g cm <sup>-3</sup> )	Sublattice occupancy		Electrical conductivity <sup>b</sup> (10 <sup>4</sup> Ω <sup>-1</sup> cm <sup>-1</sup> )	Oxidation in air (eqn. (4))			Oxidation for <i>n</i> = 1.32			Arrhenius plot	
		<i>HV</i> <sub>0.1</sub> (GPa)	<i>HV</i> <sub>0.3</sub> (GPa)		Ti (%)	N (%)		800 °C	1000 °C	800 °C	1000 °C	10 <sup>3</sup> <i>k</i>	10 <sup>4</sup> <i>k</i>	ln( <i>k</i> <sub>0</sub> )	<i>Q</i> (kJ mol <sup>-1</sup> )
		<i>n</i>	10 <sup>3</sup> <i>k</i>		<i>n</i>	10 <sup>4</sup> <i>k</i>		<i>n</i>	10 <sup>3</sup> <i>k</i>	10 <sup>4</sup> <i>k</i>	<i>n</i>	10 <sup>3</sup> <i>k</i>	10 <sup>4</sup> <i>k</i>		
0.53	0.42165(1)	23.3(14)	21.5(7)	4.866	99.3	52.6	0.48 (FC)	1.49	5.20	1.38	2.17	6.01	1.99	18.4	-211.1
0.67	0.42242(1)	24.4(16)	23.8(6)	4.986	98.8	66.2	0.52 (FC)	1.39	6.88	1.18	1.67	7.24	2.13	16.2	-190.8
0.77	0.42284(1)	22.2(09)	21.4(6)	5.127	99.5	76.6	-	-	-	-	-	-	-	-	-
0.83	0.42322(1)	20.8(11)	19.7(4)	5.218	100.0	83.0	0.94 (IN)	1.35	5.44	1.23	1.11	5.63	1.28	14.5	-177.1
0.88	0.42352(1)	-	-	5.227	99.3	87.4	0.95 (IN)	-	-	-	-	-	-	-	-
0.89	0.42353(1)	19.8(12)	19.1(4)	5.246	99.4	88.5	1.26 (IN)	1.38	4.17	1.24	0.86	4.44	0.96	14.2	-175.8
0.96	0.42387(1)	19.0(14)	17.2(5)	-	-	-	2.26 (IN)	-	-	-	-	-	-	-	-
1.00	0.42410(1)	17.2(10)	17.0(4)	5.319	98.7	98.7	3.74 (IN)	1.45	3.02	1.24	0.67	3.57	0.90	13.8	-174.3

<sup>a</sup>Figures in parentheses denote the standard deviation in the last position(s), e.g. 23.3(14) = 23.3 ± 1.4.

<sup>b</sup>FC, four-contact measurement; IN, inductive measurement.



was applied [10], where  $i$  denotes the atomic species ( $i \equiv \text{Ti, N}$ ),  $n_i$  is the number of atoms in the unit cell,  $a^3$  is the volume of the unit cell,  $\rho$  is the density,  $N_A$  is the Avogadro number,  $M_i$  is the atomic weight of species  $i$  and  $m_i$  is the mass fraction of species  $i$  in the compound.

The values for the percentage occupancy in both sublattices of  $\delta\text{-TiN}_{1-x}$  were calculated on the assumption that both sublattices can accommodate a maximum of four atoms per unit cell and that the small fraction of oxygen present in the material occupies the nitrogen sublattice. A small systematic error arises from the porosity of the samples. However, even for the most substoichiometric sample, where there were most pores in the centre, this error is much less than 1%.

The results of the occupancy analysis are presented in Fig. 5. Throughout the homogeneity region of  $\delta\text{-TiN}_{1-x}$  the occupancy of the titanium sublattice is nearly 100% whereas the occupancy of the N atoms corresponds to the composition  $[\text{N}]/[\text{Ti}]$ . This result is in agreement with the results reported by Christensen and Fregerslev [8] and Wolf [9], who measured compact samples, and Nagakura *et al.* [24], who had determined the density of powders. Generally powder determinations (a complete citation of references is given in ref. 9) show an apparent vacancy concentration of 2%–5% at the stoichiometric composition, mostly because of poor wetting of the samples by the immersion liquid. Such vacancy concentrations in the metallic sublattice are most probably present only at superstoichiometric compositions [9, 25, 26].

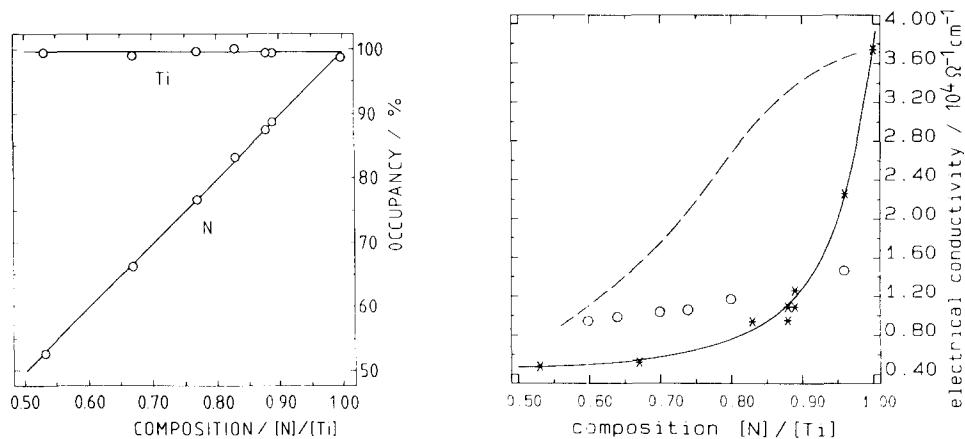


Fig. 5. Occupancy of the titanium and nitrogen sublattices *vs.* composition based on the assumption that both species can accommodate a maximum of four atoms per unit cell (NaCl lattice).

Fig. 6. Electrical conductivity of titanium nitride as a function of composition (\*, this work). Note the sharp increase in the electrical conductivity as the stoichiometric composition is approached (---, data of L'vov *et al.* from ref. 6; O, data from Aivazov *et al.* [27]; both from powder compacts).

### 3.4. Electrical conductivity

The inductive resistivity measurements on the sample plates indicated a steep increase in electrical conductivities with increasing nitrogen content. Samples at compositions with less nitrogen than  $\text{TiN}_{0.83}$  could not be measured by this technique owing to the restricted range of the apparatus. These were measured by the four-contact method. For samples higher than  $\text{TiN}_{0.89}$  the four-contact method yielded scattered results and a much lower electrical conductivity than the inductive resistivity measurements. Upon applying different currents, a current-dependent conductivity was observed in most cases for the latter samples. This is an indication that grain boundary effects or microcracks might influence the results for samples with high nitrogen contents. Since the grain sizes are only slightly different (they are slightly larger for nitrogen-rich compositions since the samples were annealed at higher temperatures), the differences in electrical conductivity most probably arise from microcracks which were introduced by the cutting and/or grinding procedure necessary to obtain bar-shaped samples from the plates. Obviously this mechanical treatment has a different impact on nitrogen-poor and nitrogen-rich samples, although no differences in the Palmqvist measurements could be detected.

The results of the electrical conductivity measurements are shown in Fig. 6 and are compared with conductivities reported for sintered powder compacts [6, 27]. The latter were the only systematic studies available covering the homogeneity range of  $\delta\text{-TiN}_{1-x}$ . Literature compilations of single values [19, 20] generally give very scattered results for the electrical conductivity of  $\delta\text{-TiN}_{1-x}$  at room temperature, with sometimes unspecified sample compositions.

The data of Lvov *et al.* (cited in ref. 6) show higher electrical conductivities at substoichiometric compositions and good agreement with the present study at the stoichiometric composition, and hence a lesser slope for the conductivity *vs.* composition curve. The data of Aivazov *et al.* [27] suggest an even more moderate slope of conductivity *vs.* composition and at stoichiometric composition do not agree with the other two sets. A similar low value at stoichiometric composition was found by Hojo *et al.* [26]. The reasons for this can be quite varied. Too high electrical conductivities at substoichiometric compositions could be attributed to the presence of nitrogen-rich surface layers on the powder particles arising from the sintering process [28]. These surface layers can be formed during the cooling period by small amounts of nitrogen in the gas phase originating either from the compacts themselves or from a nitrogen contamination in the protective gas. Too low values could be due to oxygen contamination or to too high a contact resistance between powder particles.

Interestingly,  $\text{TiC}_{1-x}$  [29] shows a very similar electrical conductivity dependence at room temperature to that found for  $\text{TiN}_{1-x}$  in the present study.

### 3.5. Oxidation behaviour

Phase analysis of the oxidation products revealed the existence of rutile ( $\text{TiO}_2$ ) as the only phase in the oxide layer at both reaction temperatures. The scales formed at 1000 °C were brownish yellow, as opposed to white at 800 °C.

The microstructures of the oxide scales generally showed a striped texture together with a recrystallized  $\text{TiO}_2$  surface layer. This was also reported by Desmaison *et al.* [30, 31] for plates of the compositions  $\text{TiN}_{0.79}$ ,  $\text{TiN}_{0.83}$  and  $\text{TiN}_{0.91}$  oxidized in pure oxygen. The stripes could be easily observed in normal light in all samples oxidized at 1000 °C. The striped texture, which originates from a periodic detachment of the scale from the substrate after a critical  $\text{TiO}_2$  layer thickness has been reached, became more predominant the lower the nitrogen content was. At 800 °C this texture phenomenon was much less pronounced. Especially at higher nitrogen contents the oxidation scale appeared speckled and only upon a near complete cross of the polarizing filters was a striped texture observable. Obviously, the higher the nitrogen content and the lower the temperature, the lower the critical thickness is before the oxide layer detaches from the nitride. This reduces the gaps between the detached layers, yielding a denser scale and an increased oxidation resistance, a quantification of which is given below.

Figure 7 shows an electron probe microanalysis (EPMA) scan for nitrogen and oxygen across the oxide scale of a sample oxidized at 800 °C. The results were corrected for the overlap of N  $K\alpha$  and Ti L1 lines [17]. Clear, sharp concentration steps occurred at the oxide–nitride interface, with no perceptible nitrogen content in the rutile scale and no perceptible oxygen content in the nitride. The latter result is interesting since it is known that  $\delta\text{-TiN}_{1-x}$  forms a complete solid solution with  $\text{TiO}$ . The very small grey interface described by Desmaison *et al.* [30], which was considered to be

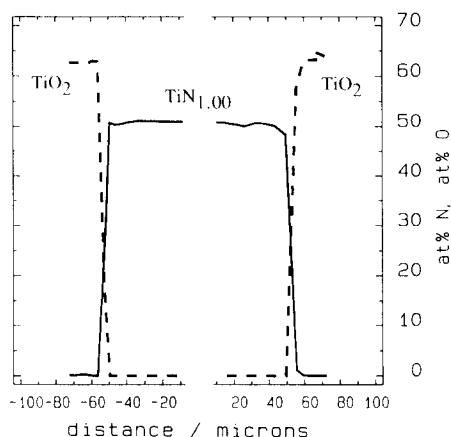


Fig. 7. Microprobe scan across the  $\text{TiO}_2$  scale and the oxide–nitride interface showing a sharp concentration jump at the oxide–nitride interface (sample oxidized at 800 °C).

titanium oxynitride, could not be observed and would probably be too thin to be determined by EPMA.

The oxidation reaction can be formulated according to



so that the mass gain upon oxidation is slightly reduced by setting the nitrogen free. For data treatment the observed mass gain was corrected on the basis of the above reaction, yielding

$$m(\text{TiO}_2) = \frac{mM_{\text{oxide}}}{M_{\text{oxide}} - M_{\text{N}}(1-x)} \quad (3)$$

where  $m(\text{TiO}_2)$  is the mass of rutile formed,  $m$  is the measured mass gain,  $M_{\text{oxide}}$  is the molar weight of rutile,  $M_{\text{N}}$  is the molar weight of nitrogen and  $1-x$  is the composition  $[\text{N}]/[\text{Ti}]$  of the titanium nitride sample  $\text{TiN}_{1-x}$ .

The mass gain as a function of temperature was treated in the form

$$m(\text{TiO}_2)^n = kt \quad (4)$$

where  $m(\text{TiO}_2)$  is the mass gain per square centimetre arising from  $\text{TiO}_2$  formation,  $n$  is an exponent,  $k$  is a rate constant and  $t$  is the time in minutes. An optimization refinement on the basis of a least-squares routine was applied in order to find the best exponent  $n$  for each data set of a specific composition at a given temperature. It should be noted that the  $n$  and  $k$  values vary with the duration of the annealing time. This is an indication that the apparent order of the reaction changes during the reaction. In the following, oxidation times up to 120 min are considered and effects occurring at longer reaction times are discussed later.

At 800 °C the exponent  $n$  is between 1.35 and 1.49 whereas at 1000 °C it is between 1.18 and 1.38. The oxidation of titanium nitride in air thus cannot be described by a parabolic law. The data sets for the two different temperatures were used to calculate the activation energy and the rate constant of the oxidation reaction according to an Arrhenius plot,  $k = k_0 \exp(-Q/RT)$ , where  $k$  is the rate constant,  $k_0$  is a pre-exponential factor and  $Q$  is the activation energy of the oxidation process.

For this treatment an average exponent  $n$  of 1.32 was calculated from the data sets of the individual mass gain functions, since only reactions of the same order, which is expressed by  $n$ , should be compared. Hence a comparison of the  $k$  values (Table 1) gives directly the relative oxidation resistance.

The data of the Arrhenius plots are given in Table 1.  $\ln(k_0)$  and  $Q$  remain approximately constant for samples higher in nitrogen content than  $\text{TiN}_{0.80}$ . The values are centred around  $\ln(k_0) = 16$  and  $Q = -191 \text{ kJ mol}^{-1}$ . This is in good agreement with the activation energy obtained by Desmaison *et al.* [30, 31] of about  $-185 \text{ kJ mol}^{-1}$  for the oxidation in pure oxygen. For samples with nitrogen contents less than  $\text{TiN}_{0.80}$  these values are higher (Table 1).

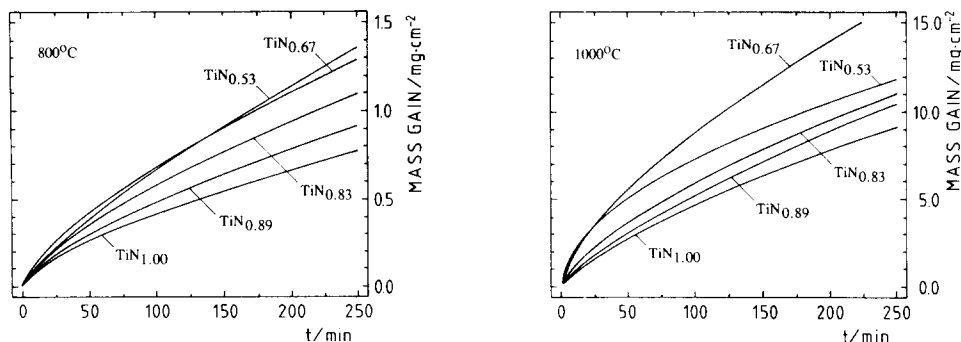


Fig. 8. Mass gain (eqn. (4)) of  $\delta$ -TiN $_{1-x}$  as a function of composition and time: top, 800 °C; bottom, 1000 °C.

From the plot of weight gain *vs.* time in Fig. 8, where longer reaction times were also taken into consideration, it is clear that the oxidation resistance increases with increasing nitrogen content of  $\delta$ -TiN $_{1-x}$  at both investigation temperatures. For the two lowest compositions the oxidation behaviour has more peculiar features. At 800 °C the oxidation rate is slower for TiN $_{0.53}$  than for TiN $_{0.67}$  at the beginning, but at longer reaction times this behaviour changes. At 1000 °C TiN $_{0.53}$  first shows a lower oxidation resistance than TiN $_{0.67}$ , followed by a higher value at longer reaction times. Metallographic investigations revealed that the sample with the lowest nitrogen content shows  $\epsilon$ -Ti $_2$ N phase formation at 1000 °C and  $\delta'$ -TiN $_{1-x}$  phase formation upon annealing at 800 °C within the nitride phase, which is consistent with the known phase reactions in the Ti-N system [3, 32]. The formation of  $\delta'$ -TiN $_{1-x}$  at 800 °C is slower (within hours) than the formation of  $\epsilon$ -Ti $_2$ N at 1000 °C (within a few minutes) [32, 33]. The oxidation times after which a cross-over of the mass gain curves occurs correspond qualitatively to the formation of these phases within the nitride phase, yielding some evidence that the oxidation resistance is increased at 1000 °C through the formation of  $\epsilon$ -Ti $_2$ N and decreased at 800 °C by the formation of  $\delta'$ -TiN $_{1-x}$  in samples of low nitrogen content.

#### 4. Conclusions

In technical applications titanium nitride with a stoichiometric composition is usually applied or proposed for application. However, this stoichiometric composition may not represent an optimum in the properties *vs.* composition function. This was, for example, stated by Hultman *et al.* [34] and Ristolainen *et al.* [35], who found better lattice matching for substoichiometric than for stoichiometric titanium nitride with the carbides of high speed steel.

## Acknowledgments

The author would like to thank Professor Peter Ettmayer for his kind support and many interesting discussions, Dr. J. Bauer for the opportunity to perform the microhardness indentation tests at the Laboratoire de Métallurgie et de Physicochimie des Matériaux, Rennes, France and Mr. M. Bohn, IFREMER, Brest for his help with the microprobe measurements. Thanks are also due to Dr. E. Bauer, Institut für Experimentalphysik, TU Vienna for making available an apparatus for the four-contact electrical resistivity measurements. Thanks are further due to Mrs. Cathryn Jelinek for help with the preparation of the manuscript. This work was supported by the Austrian National Science Foundation (FWF) under Project No. 7370 and by the French–Austrian research contract No. A16.

## References

- 1 P. Ettmayer and W. Lengauer, Nitrides, in *Ullmann's Encyclopedia of Industrial Chemistry*, Vol. A17, Verlag Chemie, Weinheim, 1991, p. 341–361.
- 2 H. A. Wriedt and J. L. Murray, *Bull. Alloy Phase Diag.*, 8 (1987) 378.
- 3 W. Lengauer, *Acta Metall. Mater.*, 39 (1991) 2895.
- 4 H. Ohtani and M. Hillert, *Calphad*, 14 (1990) 289.
- 5 E. O. Ristolainen, J. M. Molarius, A. S. Korhonen and V. K. Lindroos, *J. Vac. Sci. Technol. A*, 5 (1987) 2184.
- 6 E. Y. Vainshtein, T. S. Verkhogladova, Y. A. Zhurakovskii and G. V. Samsonov, *Fiz. Met. Metalloved.*, 12 (1961) 360.
- 7 Y. G. Tkachenko, S. S. Ordan'yan, D. Z. Yurchenko, V. K. Yulyugin and V. D. Chupov, *Izv. Akad. Nauk. SSSR, Neorg. Mater.*, 19 (1983) 1333.
- 8 A. N. Christensen and S. Fregerslev, *Acta Chem. Scand. A*, 31 (1977) 861.
- 9 T. Wolf, *Thesis*, University of Karlsruhe, 1982.
- 10 W. Lengauer and P. Ettmayer, *J. Less-Common Met.*, 109 (1985) 351.
- 11 W. Lengauer and P. Ettmayer, *Monatsh. Chem.*, 117 (1986) 275.
- 12 M. Hoch, in P. S. Rudman, J. Stringer and R. I. Jaffee (eds.), *Phase Stabilities in Metals and Alloys*, McGraw-Hill, New York, 1967, p. 419.
- 13 W. Lengauer and P. Ettmayer, *Mater. Sci. Eng. A*, 105–106 (1988) 257.
- 14 R. Täubler, S. Binder, M. Groschner, W. Lengauer and P. Ettmayer, *Mikrochim. Acta*, 107 (1992) in the press.
- 15 S. Palmqvist, *Jernkontorets Ann.*, 141 (1957) 300.
- 16 H. E. Exner, *Trans. Metall. Soc. AIME*, 245 (1969) 677.
- 17 W. Lengauer, J. Bauer, A. Guillou, D. Ansel, J.-P. Bars, M. Bohn, E. Etchessahar, J. Debuigne and P. Ettmayer, *Mikrochim. Acta*, 107 (1992).
- 18 W. Lengauer and P. Ettmayer, *High Temp.–High Press.*, 22 (1990) 13.
- 19 P. T. B. Shaffer (ed.), *High-temperature Materials*, No. 1, *Materials Index*, Plenum, New York, 1964.
- 20 L. E. Toth, *Transition Metal Carbides and Nitrides*, Academic, New York, 1971.
- 21 C. Chatfield, *Powder Metall. Int.*, 17 (1985) 113.
- 22 R. A. Andrievski and I. I. Spivak, *Strength of Refractory Compounds and Materials on Their Base (Handbook)*, Metallurgia, Chelyabinsk, 1989 (in Russian).
- 23 C. Politis and G. Rejman, *Prog. Rep. KfK-Ext. 6/78-1*, July 1978 (Kernforschungszentrum Karlsruhe).
- 24 A. Nagakura, T. Kusunoki, F. Kakimoto and Y. Hirotsu, *J. Appl. Crystallogr.*, 8 (1975) 65.

- 25 M. E. Straumanis, C. A. Faunce and W. J. James, *Acta Metall.*, 15 (1967) 65.
- 26 J. Hojo, O. Iawamoto, Y. Maruyama and A. Kato, *J. Less-Common Met.*, 53 (1977) 265.
- 27 M. I. Aivazov, I. A. Domashnev and T. V. Rezhikova, *Izv. Akad. Nauk SSSR, Neorg. Mater.*, 5 (1969) 2195.
- 28 W. Lengauer, *J. Phys. Chem. Solids*, 52 (1991) 393.
- 29 W. S. Williams, *Phys. Rev.*, 135 (1964) A505.
- 30 J. Desmaison, P. Lefort and M. Billy, *Oxid. Met.*, 13 (1979) 203.
- 31 J. Desmaison, P. Lefort and M. Billy, *Oxid. Met.*, 13 (1979) 505.
- 32 W. Lengauer, *J. Alloys Comp.*, 179 (1992) 289.
- 33 W. Lengauer and P. Ettmayer, *Rev. Chim. Miner.*, 24 (1987) 707.
- 34 L. Hultman, H. T. G. Hentzell, J.-E. Sundgren, B.-O. Johansson and U. Helmersson, *Thin Solid Films*, 124 (1985) 163.
- 35 E. O. Ristolainen, J. M. Molarius, A. S. Korhonen and V. K. Lindroos, *J. Vac. Sci. Technol. A*, 4 (1986) 1688.